RJC

RASĀYAN *J. Chem.*
Vol. 17 | No. 4 |2007-2016| October - December | 2024
ISSN: 0974-1496 | e-ISSN: 0976-0083 | CODEN: RJCABP
http://www.rasayanjournal.com
http://www.rasayanjournal.co.in

EXPLORING M^{n+}/SILICALITE-1 AS A CATALYST FOR BIGINELLI REACTION TO PRODUCE DIHYDROPYRIMIDINONE DERIVATIVES

Hery Suwito[1,✉], Lutfan Zulianto[1], Kautsar Ul Haq[1,2], Abdulloh Abdulloh[1], Erwanto Erwanto[1,3], Fitria Pebriani[1], Arjun N. Jihadi Al[1] and Taufiq-Yap Y. Hin[4]

[1]Department of Chemistry, Faculty of Science and Technology, Universitas Airlangga, Surabaya-60115, Indonesia

[2]Division of Exploration and Synthesis of Bioactive Compounds (ESBC), University CoE - Research Center for Bio-Molecule Engineering (BIOME), Universitas Airlangga, Surabaya-60115, Indonesia

[3]Department of Chemistry, Universitas Bojonegoro, Bojonegoro-62119, Indonesia

[4]Department of Chemistry, Faculty of Science, Universiti Putra Malaysia, 43400 UPM, Serdang, Selangor, Malaysia

✉Corresponding author: hery-s@fst.unair.ac.id

ABSTRACT

A series of M^{n+}/silicalite-1 was prepared to be used as a Lewis acid heterogeneous catalyst for a one-pot multicomponent Biginelli reaction. The catalysts were characterized by FTIR, XRD, NH_3-TPD, and BET. The mesoporous catalysts possess a pore diameter of 13.83 nm (138.3 Å), a surface area of 282.43 m^2/g, and a pore volume of 0.98 cm3/g, which can facilitate the transport of reactants and products smoothly during the catalytic process. Besides the acidity of the catalyst, the maximum temperature of NH_3-desorption plays an important role in the catalytic activity. Cr^{3+}/silicalite-1 showed the most active catalyst, while Zn^{2+}/silicalite-1 showed the most selective one. Besides DHPM derivatives as a major Biginelli product, C_6-styril of DHPM and Knoevenagel products were isolated if the reaction was conducted using Cr^{3+}/- and Fe^{3+}/silicalite-1. Catalyst Cr^{3+}/silicalite-1 can be used to produce DHPM attaching various substituents and showed a green catalyst potential due to its reusability capacity.

Keywords: M^{n+}/Silicalite-1, DHPM Derivatives, Biginelli Reaction, Green Catalyst.

RASĀYAN *J. Chem.*, Vol. 17, No.4, 2024

INTRODUCTION

Biginelli reaction is a popular one-pot multicomponent reaction to produce dihydropyrimidine (DHPM) derivatives using readily accessible reagents, namely benzaldehyde, ethyl acetoacetate, and (thio)urea in a protic solvent.[1] This reaction is highly considered a versatile tool for the construction of another heterocyclic scaffold, such as dihyrotetrazolopyrimidine.[2,3,4] pyrazolopyrimidine,[5] and pyranopyrimidine.[6,7] In addition, DHPM derivatives are well known for their unique pharmacological activities, such as an inhibitor of xanthine oxidase, antimicrobial, anticancer,[8] antituberculosis,[9] antioxidant,[10] anti-inflammation,[11] and anti-HIV.[12] Therefore the study and exploration of Biginelli's reaction attracted many research groups. In the classical procedure, the Biginelli reaction used to be conducted using HCl as a Brønsted acid catalyst.[1] However, in further development, DHPM derivatives have been successfully synthesized employing either homogeneous or heterogeneous catalysts with Brønsted or Lewis acid character. The application of heterogeneous catalysts is a promising alternative solution to cope with the problems that arise in the use of homogeneous catalysts.

The utilization of SiO_2 and its polymorphs become an attractive alternative to be explored. Natural SiO_2 extracted from fresh corn cob was applied successfully as a green catalyst in the Biginelli reaction to furnish 3,4-dihydropyrimidinone derivatives under solvent conditions.[13] The use of αMo-SiO_2 made using the sol-gel method for the synthesis of DHPM derivatives proceeds the reaction efficiently.[14] Heulandite type

http://doi.org/10.31788/RJC.2024.1748986

zeolite ($HTMA/CaAl_2Si_7O_{18}\cdot 6H_2O$) – a hydrophilic aluminosilicate species - was reported as an excellent catalyst for the Biginelli reaction.[15] In this paper we report our study of the application of various transition metal cations impregnated on silicalite-1 (M^{n+}/silicalite-1) as a green catalyst of Biginelli reaction to furnish DHPM. Rational consideration of the use of silicalite-1 due to its Mordenite-Framework-Inverted (MFI) structure which provides a sufficient number and dimension of pores to serve adsorption and catalytic process during the reaction so that it can be used as a supporting agent to transform homogeneous catalyst into heterogeneous one.[16] The formation of pores dimension was regulated by using two different templates, tetrapropylammonium hydroxide (TPAOH)[17]and cetyltrimethylammonium bromide (CTABr).[18]

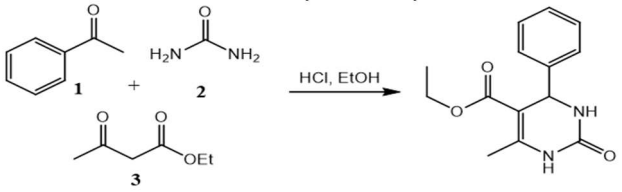

Fig.-1: Chemical Reaction of Classical Biginelli Reaction

EXPERIMENTAL

Material

All chemicals (pro analysis or pro synthesis grade) were provided from E. Merck (Darmstadt, Germany) and Sigma-Aldrich (St. Louis, Missouri, United States of America) and used without prior purification.

Preparation of Catalysts

The catalysts were prepared in two steps, those were the synthesis of silicalite-1 and followed by preparation of M^{n+}/silicalite-1. Synthesis of silicalite-1 was conducted following the available procedure[19] with slight modification. The precursor solution was prepared as follows. Tetrapropylammonium hydroxide (TPAOH), tetraethyl orthosilicate (TEOS), and water with a molar composition of 1:100:6.5 were mixed and stirred for 15 h. The mixture was aged at 80 ^{0}C for 4 days. The mesoporous solid was obtained by adding 20%wt of hexadecyltri-methylammonium bromide (CTABr) aqueous solution to the precursor solution under stirring at room temperature so that the final mixture with a molar ratio of CTABr/Si = 0.306. The mixture was then aged for 3 h at room temperature. The resulting precipitate was collected by filtration, washed with distilled water, dried at 60 ^{0}C, and finally calcined at 550 ^{0}C for 7 h. The catalysts M^{n+}/silicalite-1 were prepared by impregnation of 1 g silicalite-1 in 25 mL of 0.1 M M^{n+} salt solution for 1 day, then dried at 80 ^{0}C for 12 h.[16]

Synthesis of Molecule Targets

The mixture of urea, ethyl acetoacetate, derivatives of benzaldehyde (mol ratio is mentioned in the results), and catalyst (the amount is mentioned in the results) was put in a three-neck round bottom flask, added with 10 mL ethanol and then refluxed. The reaction progress was monitored using TLC and the reaction was stopped after completion, the product was then recrystallized with mixed solvent (*n*-hexane and ethyl acetate) to give the total yield. The product was separated by silica gel column chromatography using a suitable mobile phase as mentioned in the results.

Ethyl 4-(2,4-dimethoxyphenyl)-6-methyl-2-oxo-1,2,3,4-tetrahydropyrimidine-5-carboxylate (**4**): pale yellow crystal (0.6208g; 48.5%), m.p > 250^{o}C, R_f = 0.5 (CH_2Cl_2:ethyl acetate = 1:4); HRESI-MS $[M-H]^-$ calculated for $C_{16}H_{20}N_2O_5$ 320.1294, observed 320.1295; IR (KBr, cm^{-1}) 3239.48 (N-H), 3108.13 (C-H aromatic), 2957.14 (C-H), 1703.14 (C=O ester), 1639.89 (C=O amide), 1029.77 (C_{aryl}-O-C_{alkyl}); ^{1}H-NMR (400 MHz, $CDCl_3$) δ (ppm) 8.33 (*s*, 1H), 6.92 (*d*, *J* = 8.4 Hz; 1H); 6.43 (*d*, *J* = 2.4 Hz; 1H); 6.35 (*dd*, *J* = 2.4; 8.4 Hz, 1H); 5.74 (*s*, 1H), 5.62 (*d*, 1H), 4.04 (*q*, 2H), 3.82 (*s*, 1H), 3.76 (*s*, 1H), 2.38 (*s*, 3H), 1.09 (*t*, 3H); ^{13}C-NMR (100 MHz, $CDCl_3$) δ (ppm) 166.0; 160.6; 157.9; 148.1; 127.3; 122.6; 103.7; 98.8; 60.0; 55.5; 49.7; 18.7; 14.

Ethyl 4-(4-fluorophenyl)-6-methyl-2-oxo-1,2,3,4-tetrahydropyrimidine-5-carboxylate (**5**): white crystal (300.5 mg; 36%), R_f = 0.50 ($CHCl_3$:ethyl acetate = 1:2); HRESI-MS $[M+H]^+$ calculated for $C_{14}H_{15}FN_2O_3$ 277.0988, observed 277.0983; IR (DRS, KBr, cm^{-1}): 3122 and 3242 (N-H), 1726 (C=O

amide), 1649 (C=O ester), 1598 (C=C aromatic), 1222 (C-O-C), 792 (C-F); ^{1}H-NMR (400 MHz, $CDCl_3$) δ_H (ppm) 8.48 (s, 1H), 7.26 (dd, *J* = 8.6 and 5.4 Hz, 1H), 6.09 (s, 1H), 6.97 (d, *J* = 8.6 Hz, 1H), 5.36 (d, 1H), 4.06 (q, 2H), 1.15 (t, 3H), 2.31 (s, 3H); ^{13}C-NMR (100 MHz, CDCl3) δ (ppm) 139.7, 153.6, 128.4, 115.5, 55.1, 161.2, 101.4, 115.7, 146.5, 128.5, 165.6, 160.2, 14.3, 18.7.

Ethyl 4-(2-methoxyphenyl)-6-methyl-2-oxo-1,2,3,4-tetrahydropyrimidine-5-carboxylate (**6**): white crystal (730 mg; 77%); R_f = 0.55 ($CHCl_3$:ethyl acetate = 1:3); ^{1}H-NMR (400 MHz, $CDCl_3$) δ_H (ppm) 9.11 (s, 1H), 7.24 (s, 1H), 7.06 (m, 1H), 5.50 (d, 1H), 7.24 (m, 1H), 6.89 (m, 1H), 7.00 (m, 1H), 3.94 (q, 2H), 1.04 (s, 3H), 2.29 (s, 3H), 3.81 (s, 3H); ^{13}C-NMR (100 MHz, $CDCl_3$**)** δ (ppm) 131.3, 151.73, 156.1, 110.7, 48.5, 128.2, 100.8, 119.7, 148.4, 126.6, 164.9, 58.5, 13.6, 17.3, 54.9.

Ethyl 4-(2,5-dimethoxyphenyl)-6-methyl-2-oxo-1,2,3,4-tetrahydropyrimidine-5-carboxylate (**7**): white crystal (576 mg; 60%); R_f = 0.52 ($CHCl_3$:ethyl acetate = 1:3), HRESI-MS $[M+H]^+$ calculated for $C_{16}H_{21}N_2O_5$ 321.1450, observed 321.1451; IR (DRS, KBr, cm-1) 3113 and 3232 (N-H), 1698 (C=O amide), 1648 (C=O ester), 1493 (C=C aromatic), 1233 (C-O-C); ^{1}H-NMR (400 MHz, DMSO-*d*6) δ (ppm) 7.21 (s, 1H), 9.08 (s, 1H), 5.40 (d, 1H), 2.24 (s, 3H), 3.62 (s, 3H), 3.70 (s, 3H), 3.90 (q, 2H), 1.01 (t, 3H), 6.55 (d, *J* = 2.8 Hz, 1H), 6.77 (dd, *J* = 2.8 and 8.9 Hz, 1H), 6.88 (d, *J* = 8.9 Hz, 1H); ^{13}C-NMR (100 MHz, $CDCl_3$) δ (ppm) 153.4, 49.7, 98.1, 149.4, 14.6, 18.2, 55.8, 56.5, 59.6, 165.7, 114.6, 112.5, 112.7, 133.4, 151.3, 152.7.

Ethyl 6-methyl-2-oxo-4-(thiophen-2-yl)-1,2,3,4-tetrahydropyrimidine-5-carboxylate (**8**): white crystal (391 mg; 33%), m.p >250 °C, R_f = 0,55 (CH_2Cl_2:ethyl acetate = 1:3); HRESI-MS $[M-H]^-$ calculated for $C_{12}H_{14}N_2O_3S$ 266.0647, observed 266.0648; IR (KBr, cm^{-1}) 3242.34 (N-H), 3118.90 (C-H aromatic), 2980.02 (C-H), 1701.22 (C=O ester), 1649.14 (C=O amide); ^{1}H-NMR (400 MHz, $CDCl_3$) δ (ppm) 7.64 (s, 1H); 7.18 (*dd*, *J* = 5.0; 1.2 Hz, 1H); 6.96 (*dd*, *J* = 3.5; 1.2 Hz, 1H); 6.91 (*dd*, *J* = 5.0 Hz; 3.6 Hz, 1H); 5.76 (s, 1H); 5.69 (*d*, 1H); 4.16 (*q*, *J* = 7.2 Hz, 2H); 2.33 (*s*, 3H); 1.24 (*t*, 3H), ^{13}C-NMR (100 MHz, $CDCl_3$) δ (ppm) 169.5; 153.2; 146.6; 146.2; 126.8; 125.1; 1241; 101.9; 60.4; 50.9; 18.9; 14.3

Ethyl 4-(4-hydroxy-3-methoxyphenyl)-6-methyl-2-oxo-1,2,3,4-tetrahydropyrimidine-5-carboxylate (**9**): pale yellow crystal (936 mg; 60%), m.p = > 250°C, R_f = 0,5 ($CHCl_3$: MeOH: 9:1); HRESI-MS $[M-H]^-$ calculated for $C_{15}H_{18}N_2O_5$ 306,1137, observed 306.1126; IR (KBr, cm^{-1}) 3423.65 (O-H); 3251.98 (N-H), 3118.90 (C-H aromatic), 2953.02 (C-H), 1714.72 (C=O ester), 1678,07 (C=O amide), 1035.77 (C-O-C); ^{1}H-NMR (400 MHz, DMSO-*d*6) δ (ppm) 9.06 (*s*, 1H); 8.85 (*s*, 1H); 7.57 (*s*, 1H); 6.76 (*d*, 1H, *J* = 2 Hz); 6.66 (*d*, 1H, *J* = 8 Hz); 6.57(*dd*, 1H, *J* = 2 Hz; 8 Hz); 5.02 (*d*, 1H); 3.96 (*q*, 2H); 3.68 (*s*, 3H); 2.20 (*s*, 3H); 1.08 (*t*, 3H); ^{13}C-NMR (100 MHz, DMSO-*d*6) δ (ppm) 166.0; 152.8; 148.4; 147.8;146.3; 136.4; 118.8; 115.8; 111.4; 100.1; 59.7; 56.1; 54.1; 18.3; 14.7.

Ethyl (*E*)-4-(2,4-dimethoxyphenyl)-6-(2,4-dimethoxystyryl)-2-oxo-1,2,3,4-tetrahydropyrimi-dine-5-carboxylate (**SP-1**): pale yellow solid (38.1 mg, 28,6%); R_f = 0.57 (*n*-hexane: ethyl acetate = 1:2); HRESIMS $[M - H]^-$ calcd for $C_{25}H_{27}N_2O_7$ 467.1818, found 467.1815; IR (DRS, KBr, cm^{-1}): 3266, 3104 (str, NH amide), 2927(m, CH aliphatic), 1685 (str, C=O amide, 1607 (str, C=C conjugated), 1503 (str, C=C aromatic) dan 1270 (str, C_{aryl}-O-C_{alkyl}); ^{1}H-NMR (400 MHz, $CDCl_3$) δ_H (ppm) 8.09 (d, *J* = 17.0 Hz, 1H), 7.59 (d, *J* = 8.6 Hz, 1H), 7.30 (d, *J* = 17.0 Hz, 1H), 7.01 (d, *J* = 8.4 Hz, 1H), 6.83 (s, 1H), 6.51 (dd, *J* = 8.6, 2.3 Hz, 1H), 6.46 (d, *J* = 2.2 Hz, 1H), 6.44 (d, *J* = 2.3 Hz, 1H), 6.36 (dd, *J* = 8.4, 2.2 Hz, 1H), 5.73 (d, *J* = 2.8 Hz, 1H), 5.67 (s, 1H), 4.09 (m, 2H), 3.85 (s, 3H), 3.85 (s, 3H), 3.83 (s, 3H), 3.77 (s, 3H), 1.14 (t, *J* = 7.1 Hz, 3H); ^{13}C-NMR (101 MHz, $CDCl_3$) δ_C (ppm) 165.8, 162.2, 160.7, 158.9, 157.9, 153.1, 145.2, 128.2, 127.7, 127.5, 122.4, 117.6, 117.4, 105.6, 103.9, 99.9, 98.9, 98.4, 60.2, 55.6, 55.6, 55.5, 55.5, 50.0, 14.3.

Ethyl (*E*)-2-((*Z*)-2,4-dimethoxybenzylidene)-5-(2,4-dimethoxyphenyl)-3-oxopent-4-en-oate (**SP-2**): pale yellow oily solid (30 mg), R_f = 0.18 (n-hexane: ethyl acetate = 4:1), IR (DRS, KBr, cm-1): 1462 (C=C aromatic),1600 (C=C alkene) , and 1211 (C-O-C ether), ^{1}H-NMR (400 MHz, $CDCl_3$) δ_H (ppm): 1,27 (t, 1H, *J* = 6.9 Hz), 3.77 (s, 1H), 3.80 (s, 1H), 3.82 (s, 1 H), 3.84 (s, 1H), 4.26 (q, *J* = 7.1 Hz), 4.26 (q, *J* = 7.1 Hz), 6.36 (dd, 1H, *J* = 8.6, 2.3 Hz), 6.38 (d, *J* = 2.1 Hz), 6.40 (d, *J*=2.2 Hz), 6.47 (dd, *J* = 8.6 ; 2.3 Hz), 6.82 (d, *J* = 16.4 Hz), 7.34 (d, *J* = 8.6 Hz), 7.40 (d, *J* = 8.6 Hz), 8.19 (s, 1H), 6.82 (d, *J* = 16,4 Hz), 7.34 (d, *J*= 8.6 Hz), 7.40 (d, *J*=8.6 Hz), 8.19 (s, 1H), 6.82 (d, *J*=16.4 Hz); ^{13}C-NMR (101 MHz, CDCl3) δ_C (ppm):

14.04, 55.18, 55,28, 55.18, 55.28, 60.93, 104.73, 98.13, 97.98, 105.16, 125.34, 129.90, 130.41, 136.82, 116.36, 131.35, 141.20, 159.95, 162.63, 196.78, 159.47, 163.02.

Characterization

Catalyst

The functional group of the catalysts was determined by an FTIR spectrophotometer (IR Tracer 100, Shimadzu – Kyoto, Japan) using the diffuse reflectance method. The X-ray diffraction pattern of the sample was generated using a diffractometer (X-Ray Diffraction PANalytical Xpert PROO pode XRD) employing CuKα radiation. All samples were mounted on the sample holder, whereas the powder technique was used to determine the basal spacing. Temperature desorption programmed using NH_3 (NH_3-TPD) was used to determine the acidity of catalysts. NH_3-TPD experiments were performed on a Thermo Finnigan TPDRO 1100 apparatus equipped with a thermal conductivity detector. The experiments were conducted following available procedures.[18] Brauner-Emmer-Teller (BET) method was applied to analyze the surface characteristics of the prepared catalysts, and the analysis was conducted using Micrometrics Surface Area and Porosity Analyzer type ASAP 2020 (Micrometrics, Norcross, USA).

Molecule Targets

The reaction progress of the synthesis of molecule targets was monitored by TLC on silica gel GF_{254} aluminum sheets (0.25 mm). Separation of the reaction products was carried out on column chromatography using silica gel 60G. The infrared spectra were recorded in KBr powder on the IR spectrophotometer IRTracer 100 (Shimadzu, Kyoto, Japan) using the diffuse reflectance method. High-resolution mass spectrometer Waters LCT Premier XE (Waters, Santa Clara, CA, USA) was used to record the mass spectrum. NMR spectrometer JEOL 400 ECA (JEOL, Tokyo, Japan) was used to record the NMR spectra (^{1}H-, ^{13}C-NMR, HMQC, and HMBC), while $CDCl_3$ was used as a solvent and internal standard.

RESULTS AND DISCUSSION

Catalysts Preparation and Characterization

The prepared silicalite-1 yielded 98% and was used as supporting material, whereas the heterogenous catalysts M^{n+}/silicalite-1 were prepared by impregnation of 0.3 g silicalite-1 in the metal ion solution (0.1 M; 25 mL) under stirring for 24 h, followed by drying at 80°C for 12 h. The prepared M^{n+}/silicalite-1 catalysts were characterized based on physico-chemical analysis (FT-IR, XRD, and BET). The FTIR spectrum of the parent silicalite-1 (Fig.-2) showed vibration bands $\tilde{v}$ (cm^{-1}) at 3400 characteristics for vibration of Si-OH, 1200-1000, and 450 specific for asymmetric vibration of Si-O-Si, while symmetric vibration band of Si-O-Si appeared at 800. The infrared spectrum of all M^{n+}/silicalite-1 showed similarity with the parent silicalite-1, except the appearance of additional IR vibration bands of Zn^{2+}/silicalite-1 at $\tilde{v}$ (cm^{-1}) 1575 and 1443 indicated the carbonyl group of zinc acetate[20] which was used for the preparation of Zn^{2+}/silicalite-1.

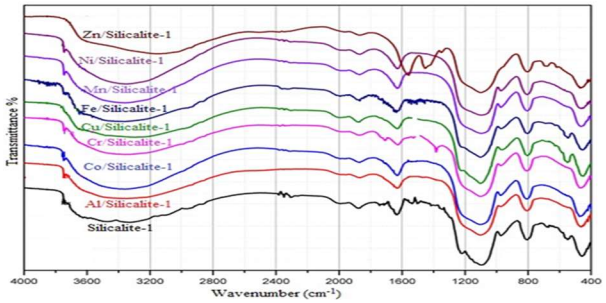

Fig.2: Infra-red Spectrum of the Prepared Catalysts

The XRD diffractogram (Fig.-3) showed an intensive peak at 2θ 24.4°, typical for silicalite-1 possessing an orthorhombic MFI structure.[21] The diffractogram of all M^{n+}/silicalite-1 exhibited similar diffraction peaks to the parent silicalite-1, except for Zn^{2+}/silicalite-1 with an additional peak at 2θ observed. This peak is typical for the crystal of $Zn(OAc)_2$ hydrate, which was used to prepare Zn^{2+}/silicalite-1 and it crystallized on the surface of silicalite-1 during the drying step after the impregnation process. The data obtained from IR and XRD proved that the impregnation process of metal cations did not build a new crystal structure

affecting the structure of supporting material silicalite-1, but they were only adsorbed on the surface of silicalite-1.

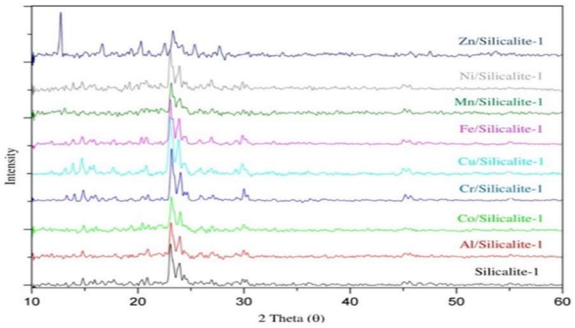

Fig.-3: XRD Diffraction Pattern of the Prepared Catalysts

The BET spectrum of silicalite-1 (Fig.-4) displayed a loop hysteresis graphical adsorption-desorption pattern, which indicated that the prepared silicalite-1 belongs to a mesoporous material.[22] In addition, the BET experiment informed that the prepared silicalite-1 possessed a pore diameter of 13.83 nm (138.3 Å), a surface area of 282.43 m^2/g, and a pore volume of 0.98 cm^3/g. Based on a computational calculation using HyperchemTM release 8.0.8 for the Windows Molecular Modelling system, it was found that the dimension of the target molecule (Comp 4) is 10.6 Å length and 9.6 Å width. Considering the dimension of the catalyst pore and the size of the reaction product, it is obvious that the porous catalyst can facilitate the transport of reagents and products during the catalytic process smoothly.

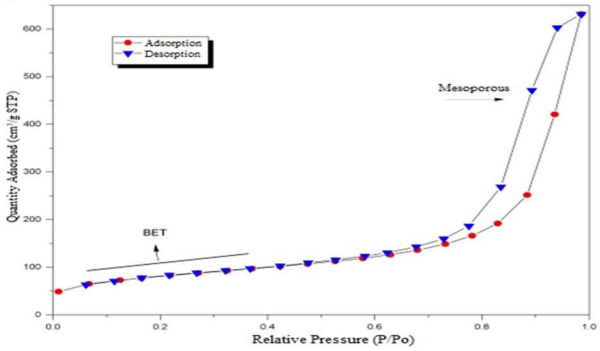

Fig.-4: Adsorption-Desorption Pattern of BET Experiment of Silicalite-1

The acidity and acid site distribution of the prepared catalysts were evaluated by the ammonia-temperature-programmed desorption (NH_3-TPD) experiment. The NH_3-TPD profiles and amount of acidity of catalysts are displayed in Fig.-5 and Table-1 respectively. The NH_3-TPD profiles exhibited NH_3 desorption peaks at temperatures ranging from 100 to 950°C and a typical peak temperature for each catalyst. Based on the NH_3-desorption range temperature, a peak at a temperature below 250°C is classified as weak, in the range of 250-400°C is considered moderate, while a peak higher than 400°C is classified as strong acid.[23] Silicalite-1 showed a broad desorption peak with mainly medium acid at 280°C, whereas other catalysts showed more than one desorption peak with typical peak temperature, whether as a weak, medium, or strong acid. The Zn^{2+}/silicalite-1 exhibited as a strong acid with a desorption peak at 831°C and 0.51 mmol/g NH_3 was desorbed, whereas Cr^{3+}/silicalite-1 showed as a strong acid with two desorption peaks at 527 and 708°C, where 0.58 mmol/g and 1.03 mmol/g NH_3 was desorbed respectively.

Effect of Catalyst Acidity Toward Catalytic Activity

Eight M^{n+}/silicalite-1 catalysts were prepared, whereas silicalite-1 was used as supporting material. As a reaction model to study the catalyst performance, we synthesized compound 4 from the reaction between 2,4-dimethoxy benzaldehyde 1, urea 2, and ethyl acetoacetate 3 in a mol ratio of 5:6:5, using ethanol as solvent. The yields are displayed in Table-1. As shown in Table-1, acid strength played an important role in the product formation. Catalysts with only medium strength formed no product (entry 1), and only catalysts with strong acid character gave the product (entry 2-9).

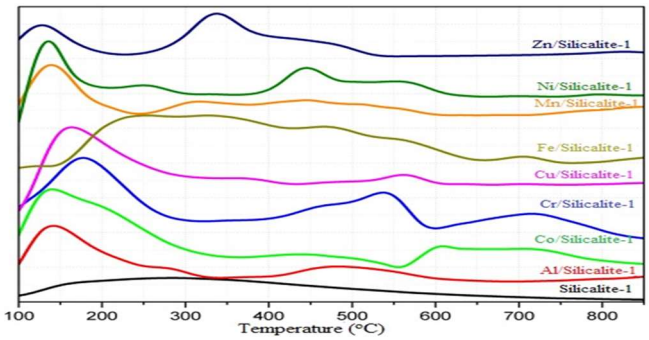

Fig.-5: NH3-TPD Profiles of the Catalysts Under Different Temperatures

Table-1: The Acidity of the Prepared Catalysts and Effect of Acid Strength Toward the Reaction Yield

Entry	Catalyst	T_{max} (°C)	Bolis acidity	Total acid sites (mmol/g)	Strong acid site (mmol/g)	Total Yield (%)
1	Silicalite-1	280	medium	10.29	0	0
2	Al^{3+}/silicalite-1	131	weak	1.44	0.63	37
		464	strong	0.63		
3	Co^{2+}/silicalite-1	138	weak	10.74	1.01	59
		708	strong	1.01		
4	Cr^{3+}/silicalite-1	169	weak	1.60	1.61	75.6
		527	strong	0.58		
		708	strong	1.03		
5	Cu^{2+}/silicalite-1	151	weak	3.56	0.91	24
		572	strong	0.91		
6	Fe^{3+}/silicalite-1	346	medium	3.55	2.18	69.8
		466	strong	2.18		
7	Mn^{2+}/silicalite-1	146	Weak	1.97	0.44	12
		454	strong	0.44		
8	Ni^{2+}/silicalite-1	130	weak	1.87	1.81	32.7
		235	weak	0.66		
		444	strong	1.03		
		538	strong	0.78		
9	Zn^{2+}/silicalite-1	125	Weak	3.84	0.51	32
		336	medium	9.36		
		831	strong	0.51		

Cr^{3+}/silicalite-1 (entry 4) with the highest peak temperature gave the best result although it had less number of total strong acid sites compared to Fe^{3+}/silicalite-1 (entry 6) and Ni^{2+}/silicalite-1 (entry 8). Therefore we assumed that maximum desorption temperature (T_{max}) is the next factor affecting the yield besides strong acid sides. This finding is in accordance with the statement of Ding and Zhao[26] that a catalyst with stronger acidity produces more products. Cr^{3+}/silicalite-1 was then used for further experiments to study the effect of catalyst dosage on the product (comp. **4**) using the same ratio of reactant (5:6:5) and the results are presented in Fig.-**6**. The experiment showed that maximum yield was obtained by using of 0.10 g catalyst. A decrease in yield was observed by the usage of more amount of catalysts. This observation indicated that usage of more than 0.10 g catalysts caused an inhibitory effect on the product formation.

The mol ratio of reactants was the next parameter to be studied, and the results are presented in Table-2. As shown in Table-2, the maximum yield was obtained in the reaction using an almost equivalent mol ratio of reactants (entry-8). This observation is in accordance with statement of[24] that the Lewis acid-catalyzed Biginelli reaction proceeds stoichiometrically in an equivalent ratio between the reactants.

Catalyst Reusability

Besides stability, the reusability of a catalyst is one of the most important features of a catalyst that should be considered in industrial usage and in environmental issues. After completion of the reaction, the catalysts

(Cr^{3+}/silicalite-1 and Fe^{3+}/silicalite-1 were recovered by washing it with ethanol and dried, then reused. The results are presented in Fig.-7 and showed that after three times, its activity reduced slightly.

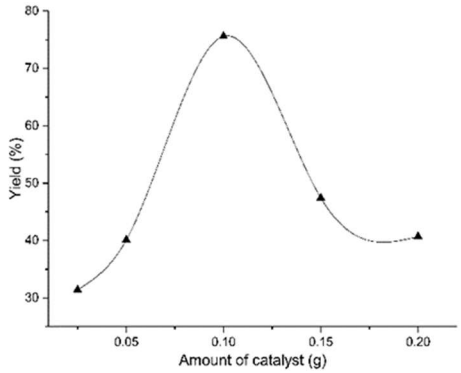

Fig.-6: Effect of Catalyst Amount on the Reaction Yield

Table-2: Correlation of Mol Ratio Reactants to the Yield

Catalyst	Entry	Mol ratio of reactant (mmol)			Total yield (%)
		2,4-dimethoxy benzaldehyde	urea	Ethyl acetoacetate	
Cr^{3+}/silicalite-1 (0.1 g)	1	1	4	1	32.3
	2	1	4	2	47.8
	3	1	4	3	48.5
	4	2	4	1	43.9
	5	2	4	3	68.1
	6	3	4	1	73.3
	7	3	4	2	68.9
	8	5	6	5	75.6

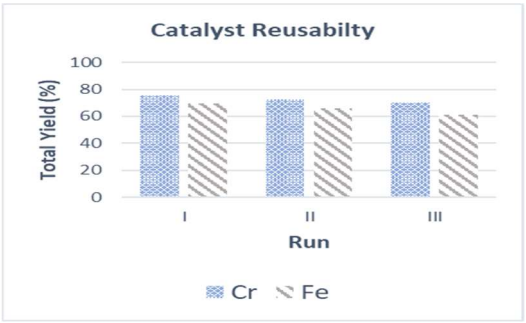

Fig.-7: Reusability of Cr^{3+}/Silicalite-1 and Fe^{3+}/Silicalite-1 for the Synthesis Comp. 4

Selectivity of Catalyst

To observe the selectivity of catalysts, we performed a TLC analysis and concluded that reaction products of all catalysts showed two spots with R_f values of 0.58 and 0.30 ($CHCl_3$:ethyl acetate = 3:1), except Zn^{2+}/silicalite-1 gave only one spot with R_f 0.30, which mean that Zn^{2+}/silicalite-1 is the most selective one. The crude products were then subjected to silica column chromatography for separation using $CHCl_3$: ethyl acetate = 3:1 as mobile phase, and the results are presented in Table-3.

Table-3: Main and Side Product of Biginelli Reaction Using Prepared Catalysts

Catalyst	Total yield (g)	Compound 4 (g)	Side Product (g)
Al^{3+}/silicalite-1	0.5920	0.4089	0.0058
Co^{2+}/silicalite-1	0.9440	0.5019	0.0038
Cr^{3+}/silicalite-1	1.2096	0.7481	0.0381
Cu^{2+}/silicalite-1	0.3840	0.1539	0.0017
Fe^{3+}/silicalite-1	1.1168	0.7323	0.0294
Mn^{2+}/silicalite-1	0.1920	0.1454	0.0019

Ni^{2+}/silicalite-1	0.5232	0.3929	0.0072
Zn^{2+}/silicalite-1	0.0932	0.0932	--

Subsequently, we tested the purity of the side products using TLC with three different mobile phases, and the results are presented in Table-4.

Table-4: Purity Test of Side Product using TLC Experiment

Catalyst	R_f (*n*-hexane: ethyl acetate)						
	1:1		4:1			2:3	
Al^{3+}/silicalite-1	0.67	0.75	0.18	0.29	0.34	0.56	0.64
Cr^{3+}/silicalite-1	0.67	0.75	0.18	0.29	0.34	0.56	0.64
Cu^{2+}/silicalite-1	0.67	0.75	0.18	0.29	0.34	0.56	0.64
Fe^{3+}/silicalite-1	0.67	0.75	0.18	0.29	0.34	0.56	0.64
Mn^{2+}/silicalite-1	0.67	0.75	0.18	0.29	0.34	0.56	0.64
Ni^{2+}/silicalite-1	0.33		0.00			0.08	

As presented in Table-4, catalyst Ni^{2+}/silicalite-1 showed 1 spot (compound SP-1), while other catalysts exhibited 3 spots (n-hexane: ethyl acetate = 4:1). Due to the limited amount, in this experiment we explored further the side product obtained from the catalyst Cr^{3+}/silicalite-1 and Fe^{3+}/silicalite-1 and focused on the spot of R_f 0.18 (compound SP-2). Based on the spectroscopy data, revealed that SP-1 is (*E*)-4-(2,4-dimethoxyphenyl)-6-(2,4-dimethoxystyryl)-2-oxo-1,2,3,4-tetrahydropyrimidine-5-carboxylate, whereas SP-2 is ethyl (*E*)-2-((Z)-2,4-dimethoxy-benzylidene)-5-(2,4-dimethoxyphenyl)-3-oxopent-4-enoate. The proposed reaction pathway of main product and side product formation is presented in Fig.-8.

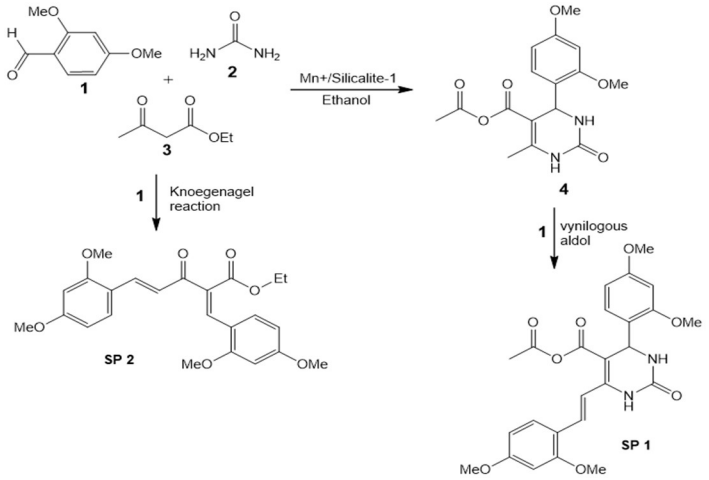

Fig.-8: Proposed Reaction Pathway of the Main and Side Products (SP) Formation

Application of Cr^{3+}/Silicalite-1 for the Synthesis of DHPM Derivatives

The optimum reaction condition was then applied to synthesize a series of DHPM derivatives. The synthesis was carried out by reaction of ethyl acetoacetate, urea, and a series of derivatives of benzaldehyde, and the results are presented in Table-5.

The results of synthesis showed that catalyst Cr^{3+}/silicalite-1 can be applied for the synthesis of DHPM derivatives using various kinds of benzaldehyde derivatives possessing electron donating group, electron-withdrawing group, or heteroaromatic. Benzaldehyde with an electron-donating substituent gave a better yield than with an electron-withdrawing substituent.

Table-5: The Results of DHPM Derivatives Synthesis using Cr^{3+}/Silicalite-1 as Catalyst

Entry	Aromatic aldehyde	Yield (%)
1 (compd 5)		36

2 (comp 6)		77
3 (compd 7)		60
4 (compd 8)		33
5 (compd 9)		60

CONCLUSION

In this present study, eight catalysts of M^{n+}/silicalite-1 have been successfully synthesized and their catalytic performances in the Biginelli reaction to furnish DHPM derivatives have been investigated. Cr^{3+}/silicalite-1 showed the best performance among other catalysts. Besides its acidity strength, the peak temperature of NH_3 desorption, amount of catalyst, and mol ratio of reactants are also important factors for the yield. Two side products as a result of aldol type and double Knoevenagel reaction were isolated respectively.

ACKNOWLEDGMENTS

The authors acknowledge Universitas Airlangga for the research funding through the "Hibah Riset Mandat 2019 research scheme", grant no.1408/UN3/2019.

CONFLICT OF INTERESTS

The authors declare that there is no conflict of interest.

AUTHOR CONTRIBUTIONS

All the authors contributed significantly to this manuscript, participated in reviewing/editing, and approved the final draft for publication. The research profile of the authors can be verified from their ORCID ids, given below:

Hery Suwito http://orchid.org/0000-0002-5844-067x
Lutfan Zulianto http://orchid.org/0009-0001-9588-0279
Kautsar Ul Haq http://orchid.org/0000-0002-0584-5040
A.Abdulloh http://orchid/0000-0001-9149-2028
E. Erwanto http://orchid/0000-0002-1043-6049
Fitria Pebriani http://orchid/0009-0008-3616-410X
Arjun Niam Jihadi Alhttp://orchid/0000-0002-7550-3193
Yun Hin Taufiq-Yap http://orchid/0000-0002-3994-6720

REFERENCES

1. G.C.Tron, A. Minassi, G. Appendino, *European Journal Organic Chemistry*, **2011(28)**, 5541(2011), https://doi.org/10.1002/ejoc.201100661
2. H. Murata, H. Ishitani, M. Iwamoto, O*rganic & Biomolecular Chemistry*, **8**, 1202(2010), https://doi.org/10.1039/B920821F
3. H. Suwito1, N. Kurnyawaty, K.U. Haq, R. Ramadhan, A. Abdulloh, H.D. Hardiyanti, P. Phuwapraisirisan, *Rasayan Journal of Chemistry*, **16(1)**, 147(2023), http://doi.org/10.31788/RJC.2023.1618025

4. R. Javahershenas, H. Mei, M. Koley, V.A. Soloshonok, A. Makarem, *Synthesis*, **56(16)**, 2445(2024), https://doi.org/10.1055/s-0042-1751526
5. A. Chandravarkar, T. Aneeja, G. Gopinathan, *Journal of Heterocyclic Chemistry*, **61(1)**, 5(2023), https://doi.org/10.1002/jhet.4742
6. M.P. Parmar, R.M. Vala, H.M. Patel, *ACS Omega*, **8(2)**, 1759(2023), https://doi.org/10.1021/acsomega.2c05349
7. Z. Balali, J. Safaei-Ghomi, E. Mashhadi, *Scientific Reports*, **14**, 14810(2024), https:doi.org/10.1038/s41598-024-65519-x
8. B. Zhang, Y. Duan, Y. Yang, Q. Mao, F. Lin, J. Gao, X. Dai, P. Zhang, Q. Li, J. Li, R. Dai, S. Wang, *European Journal of Medicinal Chemistry*, **227**, 113928(2022), https://doi.org/10.1016/j.ejmech.2021.113928
9. M.S. El-Shoukrofy, A. Atta, S. Fahmy, D. Sriram, .G. Shehat, I.M. Labouta, M.A. Mahra, *Journal of Enzyme Inhibiton and Medicinal Chemistry*, **39(1)**, 2386668(2024), https://doi.org/10.1080/14756366.2024.2386668.
10. A.M. Hantosh, N.A. Rajab, F.T. Abachi, *Eurasian Chemical Communications*, **5(3)**, 216(2023), https://doi.org/10.22034/ECC.2023.346409.1489
11. B.M. Facchin, T.L. Lubschinski, Y.J.K Moon, P.G.F. de Oliveira, B.K. Beck, Z. da Silva Buss, L.A.E Pollo, M.W. Biavatti, L.P. Sandjo, E.M. Dalmarco, *Fundamental Clinical Pharmacology*, **38(1)**, 168(2024), https://doi.org/10.1111/fcp.12945
12. J. Senapathi, A. Bommakanti, V. Kusuma, S. Vangara, A.K. Kondapi, Bioorganic & Medicinal Chemistry, **52**, 116526(2021), https://doi.org/10.1016/j.bmc.2021.116526
13. S. Khamsan, C. Janya, J. Chanawongsa, N. Injan, W. Keawmesri, M. Jaimasith, C. Jitmanee, *International Journal of Science*, **17(1)**, 32(2020),
14. K. Kouachi, G. Lafaye, S. Pronier, L. Bennini, S. Menad, *Journal of Molecular Catalysis A: Chemical*, **395**, 210(2014), https://doi.org/10.1016/j.molcata.2014.08.025
15. M. Tajbakhsh, B. Mohajerani, M.M. Heravi, A.N. Ahmadi, *Journal of Molecular Catalysis A: Chemical***, 236**, 216(2005), https://doi.org/10.1016/j.molcata.2005.04.033
16. M.W. Khalil, M. Abdel Rahim, A. Zimmer, H.B. Hassan, R.M. Abdel-Hameed, *International Journal of Electrochemical Science*, **144**, 35(2005), https://doi.org/10.1016/S1452-3981(23)07755-6
17. X-S. Wang, X-W. Guo, G. Li, *Catalysis Today*, **74(1–2)**, 65(2002), https://doi.org/10.1016/S0920-5861(01)00531-4
18. S. Smitha, P. Shajesh, P.R. Aravind, S.R. Kumar, P.K. Pillai, K.G.K. Warrier, *Microporous and Mesoporous Material*, **91(1-3)**, 286(2006), https://doi.org/10.1016/j.micromeso.2005.11.051
19. G.A. Eimer, I. Dı´az, E. Sastre, S.G. Casuscelli, M.E. Crivello, E.R. Herrero, J. Perez-Pariente, Applied Catalysis A: General. **343**, 77(2008), https://doi.org/10.1016/J.apcata.2008.03.028
20. Y.H. Taufiq-Yap, H.V. Lee, M.Z. Hussein, R. Yunus, *Biomass and Bioenergy*, **35(2)**, 827(2011), https://doi.org/10.1016/J.biombioe.2010.11.011
21. A.C. Tella, G. Mehlana, L.O Alimi, S.A. Bourne, Zeitschrift fur Anorganische und Allgemeine Chemie, **643(8)**, 523(2017), https://doi.org/10.1002/zaac.201600460
22. A. Zecchina, S. Bordiga, G. Spoto, L. Marchese, G. Petrini, G. Leofanti, M. Padovan, M, *Journal Physical Chemistry*, **96(12)**, 4985(1992), https://doi.org/10.1021/j100191a047
23. S. Lowell, J.E. Shields, M.A. Thomas, M. Thommes, Characterization of Porous Solids and Powders: Surface Area, Pore Size, and Density. Kluwer Academic Publishers, Dordrecht, p. 78,91 (2004).
24. V. Bolis, Calorimetry and Thermal Methods in Catalysis. Springer-Verlag Berlin Heidelberg, pp. 112-125 (2013)
25. H. Nagarajaiah, A. Mukhopadhyay, J.N. Moorthy, *Tetrahedron Letter*, **57(47)**, 5135(2016), https://doi.org/10.1016/j.tetlet.2016.09.047
26. D. Ding, C.G. Zhao, *European Journal of Organic Chemistry*, **20**, 3802(2010), https://doi.org/10.1002/ejoc.201000448

[RJC- 8986/2024]